



Determination of the parameters affecting electrospun chitosan fiber size distribution and morphology

V. Sencadas^{a,*}, D.M. Correia^b, A. Areias^a, G. Botelho^b, A.M. Fonseca^b, I.C. Neves^b, J.L. Gomez Ribelles^{c,d,e}, S. Lanceros Mendez^a

^a Centro/Departamento de Física, Universidade do Minho, Campus de Gualtar, 4710-058 Braga, Portugal

^b Dept. Química, Centro de Química, Universidade do Minho, Campus de Gualtar, 4710-057 Braga, Portugal

^c Centro de Biomateriales e Ingeniería Tisular, Universidad Politécnica de Valencia, Camino de Ver s/n, 46022 Valencia, Spain

^d Centro de Investigación Príncipe Felipe, Autopista del Saler 16, 46013 Valencia, Spain

^e CIBER en Bioingeniería, Biomateriales y Nanomedicina, Valencia, Spain

ARTICLE INFO

Article history:

Received 23 May 2011

Received in revised form 9 July 2011

Accepted 6 September 2011

Available online 12 September 2011

Keywords:

Chitosan
Electrospinning
Nanofiber
Processing

ABSTRACT

The production of chitosan nanofiber mats by electrospinning presents serious difficulties due to the lack of suitable solvents and the strong influence of processing parameters on the fiber properties. Two are the main problems to be solved: to control the properties of the solution in order to obtain large area uniform fiber mats by having a stable flow rate and to avoid sparks during the process, damaging the fiber mats. In this work chitosan electrospun mats have been prepared from solutions of trifluoroacetic acid/dichloromethane mixtures, allowing solving the aforementioned problems. Mats with uniform fibers of submicron diameters without beads were obtained. Further, the influence of the different solution and process parameters on the mean fiber diameter and on the width of the distribution of the fiber sizes has been assessed. Solvent composition, needle diameter, applied voltage and traveling distance were the parameters considered in this study.

© 2011 Elsevier Ltd. All rights reserved.

1. Introduction

Increasing attention has been given in recent years to natural polymers, such as polysaccharides, due to their abundance in nature, unique structures and characteristics with respect to synthetic polymers (Honarkar & Barikani, 2009). Chitosan is a natural linear polysaccharide composed of glucosamine and N-acetyl glucosamine units linked by $\beta(1-4)$ glycosidic bonds. Although naturally present in some microorganisms and fungi, commercial chitosan is industrially produced by partial deacetylation of chitin by removal of acetamide groups. Chitin is the second most abundant natural polysaccharide after cellulose. It is mainly found in crustacean shells (shrimp, crab, etc.), insect cuticle and cell walls of fungi (Baldrick, 2010; Fernandez-Megia, Novoa-Carballal, Quiñoá, & Riguera, 2005; Krajewska, 2005; Malafaya, Silva, & Reis, 2007; Ravi Kumar, 2000). The degree of deacetylation, DD, which defines the distinction between chitin and chitosan, is not precisely established. The term chitosan is found in the literature to describe polymers of chitosan with different molecular weights, viscosity

and degree of deacetylation (40–98%) (Baldrick, 2010). However, the term chitosan is generally applied when the degree of deacetylation is above 70% and the term chitin is used when the degree of deacetylation is below 20% (Baldrick, 2010).

Chitosan in its crystalline form is usually insoluble in aqueous solutions above a pH of ~ 7 . However, due to the existence of primary amine groups, the structure can be protonated and the protonated free amine groups on glucosamine facilitate the solubility of the molecule, being therefore highly soluble in acid pH (Pillai, Paul, & Sharma, 2009; Yaghobi & Hormozi, 2010).

Chitosan offers many structural possibilities for chemical modifications in order to induce novel properties, functions and applications, in particular in the biomedical area. It is nontoxic, biocompatible and biodegradable and therefore an excellent material for biomedical applications (Jayakumar, Menon, Manzoor, Nair, & Tamura, 2010; Jayakumar, Prabakaran, Nair, & Tamura, 2010; Jayakumar, Prabakaran, Nair, Tokura, et al., 2010; Jayakumar, Prabakaran, Sudheesh Kumar, Nair, & Tamura, 2011).

Recently, much attention has been paid to chitosan based nanofibers as biomaterial. There are several methods for the fabrication of nanofibers, making use of chemical, thermal and electrostatic principles (Beachley & Wen, 2010). The polymer nanofiber fabrication methods most commonly associated with

* Corresponding author. Tel.: +351 253 604 320.

E-mail address: vsencadas@fisica.uminho.pt (V. Sencadas).

biomedical applications are electrospinning, self-assembling, peptide reactions and phase separation. The electrospinning process has attracted much attention for the production of polymer fibers as it can produce them with diameters in the range from several micrometers down to tens of nanometers, depending on the polymer and processing conditions (Jayakumar, Menon, et al., 2010; Jayakumar, Prabakaran, Nair, Tokura, et al., 2010; Jayakumar et al., 2011). The nanofibers produced by this technique are formed from a liquid polymer solution or melt that is feed through a capillary tube into a region of an electric field generated by connecting a high voltage power source to the capillary tube.

Chitosan nanofibers were successfully prepared by Ohkawa, Cha, Kim, Nishida, and Yamamoto (2004). The authors studied the solvent effect on the morphology of electrospun chitosan nanofibers by varying chitosan relative concentration with different solvents. The solvents tested were diluted hydrochloric acid, acetic acid, formic acid and trifluoroacetic acid (TFA). It was found that when the concentration of chitosan increased, the morphology of the deposited fibers on the collector changed from spherical beads to an interconnected fibrous system. Further, the addition of dichloromethane (DCM) to the chitosan/TFA solution improved the homogeneity of the electrospun chitosan nanofibers. Electrospinning conditions were optimized in order to obtain homogeneous chitosan nanofibers with an average diameter of 330 nm. Other studies on electrospun chitosan nanofibers have been also reported (Jayakumar, Menon, et al., 2010; Jayakumar, Prabakaran, Nair, Tokura, et al., 2010; Jayakumar et al., 2011). Schiffman and Schauer (2006, 2007) obtained bead-free electrospun chitosan nanofibers from a solution of TFA and chitosan with different molecular weights. A small correlation between viscosity and fiber diameter was found. Despite these efforts, large fiber mats with controlled fiber dimensions are not obtained mainly due to the large electrical conductivity of the TFA solvent, which leads to an unstable process in which the flow rate is controlled by the electric field more than by the dispenser. Further, electrical sparks often occur, damaging parts of the samples. In fact, almost no cell cultures have been reported until now in pure chitosan electrospun fiber mats (Jayakumar, Menon, et al., 2010; Jayakumar, Prabakaran, Nair, Tokura, et al., 2010; Jayakumar et al., 2011).

The electrospinning technique is very versatile and a wide range of parameters can play an important role in obtaining the desired nanofiber size and microstructure. These parameters include solution viscosity, voltage, feed rate, solution conductivity, capillary-to-collector distance and capillary tube size (Bhardwaj & Kundu, 2010; Sill & von Recum, 2008). In this work, a systematic study has been performed in order to solve the aforementioned main problems. By controlling solution parameters a stable process has been achieved allowing obtaining large fiber mats with tailored fiber dimension. Further, the effect of the main processing parameters such as solvent concentration, flow rate, applied voltage, feed rate and inner needle diameter on the chitosan fiber characteristics and sample morphology has been studied in order to set the ground for a systematic and reproducible way to obtain chitosan nanofiber samples for specific applications.

2. Experimental

2.1. Materials

Chitosan practical grade polymer was purchased from Sigma–Aldrich with $\geq 75\%$ degree of D-acetylation. Dichloromethane (DCM) and trifluoroacetic acid (TFA, 99% ReagentPlus) were purchased from Sigma–Aldrich (Table 1). All materials were used as received from the provider.

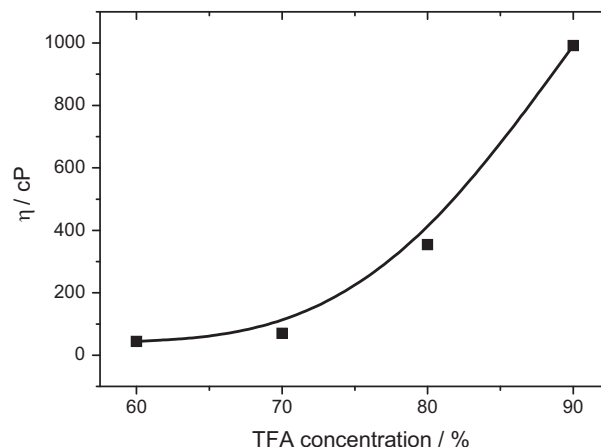


Fig. 1. Variation of the viscosity of the polymer solution with varying TFA/DCM ratio. The line is just a guide for the eyes.

2.2. Preparation of the solution

The polymer was dissolved in a TFA/DCM solution with different TFA/DCM volume ratios for a 7% (weight/volume) of chitosan. The solution were prepared under a constant and vigorous magnetic stirring (JPSelecta, Agimatic-E) at room temperature until complete dissolution of the chitosan. The viscosity of the prepared solutions was measured in a Viscostar Plus set-up from Fungilab. The variation of the viscosity of the polymer solution with varying TFA/DCM ratio is represented in Fig. 1.

2.3. Electrospinning

The polymer solution was placed in a commercial plastic syringe fitted with a steel needle. The inner diameter of the needle was 0.5, 1.0 and 1.7 mm for different experiments. Electrospinning was conducted by applying a voltage ranging from 20 to 30 kV with a PS/FC30P04 power source from Glassman. A syringe pump (Syringepump) fed the polymer solution into the tip at a rate between 1 and 8 ml h⁻¹. The electrospun samples were collected on a grounded collecting plate placed at different distances from 50 to 200 mm from the needle tip.

2.4. Characterization

Electrospun fibers were coated with a thin gold layer using a sputter coater from Polaron (SC502) and the morphology of the membranes were observed by scanning electron microscopy (SEM, JSM-6300 from JEOL) at an accelerating voltage of 15 kV. The fiber diameter distribution was calculated over 50 fibers with the Image J software (Image J, 2011) from the SEM images obtained at a magnification of 3500 \times .

The degree of deacetylation was determined by nuclear magnetic resonance (NMR) according to the procedure described in Fernandez-Megia, Novoa-Carballal, Quiñoá and Riguera (2005). Five milligram of chitosan after and before electrospun were added to a 5 mm NMR tube containing 0.5 ml of 2% deuterium chloride (DCI, from Fluka) solution in deuterated water (D₂O, Mw = 20.02, ACROS Organics) and heated at 70 °C for 1 h in order to speed up the dissolution. The results for the ¹H NMR were collected in a Varian Unity Plus 300 at 70 °C.

3. Results and discussion

Several parameters affect the fiber morphology and size distribution of the polymer electrospun fibers. Among the most

Table 1

Properties of the solvents used in the present work (Budavari, 1996).

Solvent	Melting point (°C)	Boiling point (°C)	Density (g cm ⁻³)	Dipole moment (Debye)	Dielectric constant
TFA	-15.2	73.0	1.535	2.28	8.42
DCM	-95.1	40.0	1.327	1.60	8.93

important ones are those corresponding to the initial polymer solution: parameters related to the solvent used (dielectric constant, volatility, boiling point and others), the solution concentration (that controls the viscosity) and the molecular weight of the polymer (that allows polymer entanglement). The main parameters that control the jet formation and solvent evaporation rate are the feed rate through the needle and needle diameter, traveling distance from the needle to the collector, temperature and electric field (Ramakrishna, Fujihara, Teo, Lim, & Ma, 2005; Ribeiro, Sencadas, Ribelles, & Lanceros-Méndez, 2010; Teo & Ramakrishna, 2006).

TFA is a strong acid that can dissolve the polymer through the formation of salts that destroy the strong interactions that exist between the molecules of chitosan (Ohkawa, Cha, Kim, Nishida, & Yamamoto, 2004). The salt formation occurs between the TFA and the amino groups along the chitosan chain after the following sequential steps: first, protonation of amine groups ($-NH_2$) along the chain of chitosan; second, ionic interaction between protonated amino groups ($-NH_3^+$) and then formation of trifluoroacetate anions. In this configuration, the salts are soluble in an aqueous media. In the present work, chitosan was dissolved in a TFA/DCM blend with different TFA/DCM ratios (Fig. 1) in order to control the viscosity and conductivity of the final solution (Table 1). These parameters have strong influence in the electrospinning process and therefore in the final fiber morphology. The SEM images for the electrospun samples obtained from a solution of chitosan with different TFA/DCM volume ratios and fixed traveling distance of 150 mm, needle diameter of 0.5 mm, flow rate of 2 ml h⁻¹ and a voltage of 25 kV are presented in Fig. 2.

Schiffman et al. reported that electrospinning of chitosan in pure TFA solvent was viable for lower chitosan concentrations (2.7%, w/v) (Schiffman & Schauer, 2006, 2007). In the present work, it was difficult to stabilize the electrospinning process for TFA/DCM

concentrations rich in TFA solvent (higher than 80% TFA) in the solution due to the presence of sparks that frequently appeared during the fiber processing, even for small applied electric fields, therefore hindering the electrospinning process. An increase of TFA in the solution increases the viscosity (Fig. 1) and the conductivity of the medium, which are at the origin of the sparks. Electrospinning involves stretching of the solution caused by the repulsion of the charges at its surface. If the conductivity of the solution is increased, more charges can be carried out by the electrospinning jet. The free amines trifluoroacetate anions formed during the chitosan dissolution in TFA increase the conductivity of the solution (Dannhauser & Cole, 1952) and, therefore, the critical voltage for electrospinning to occur is reduced.

Further, for TFA/DCM solvent mixtures with low TFA content, the dissolution of the polymer was extremely difficult and during the electrospinning process some drops fell from the needle due to the lower viscosity of the solution. These drops completely dissolved the formed fiber and destroyed the homogeneity of the electrospun mats. It was also observed that the average fiber diameter of the electrospun mats decreased with increasing DCM content in the solvent mixture. On the other hand, a larger fiber size distribution was observed with increasing TFA content in the solution (Fig. 3).

Fig. 3 was obtained from histograms analogous to those shown in Fig. 2 (the ones corresponding to Fig. 2c and d are included in Fig. 3), from which the mean value was calculated. The bars in Fig. 3 indicate the average and the standard deviation of the fiber diameters.

The influence of the inner diameter of the needle in the average size of the electrospun fibers was characterized. For the samples processed with a needle with an inner diameter of 0.5 mm, the presence of very thin fibers with diameter ~250 nm was observed.

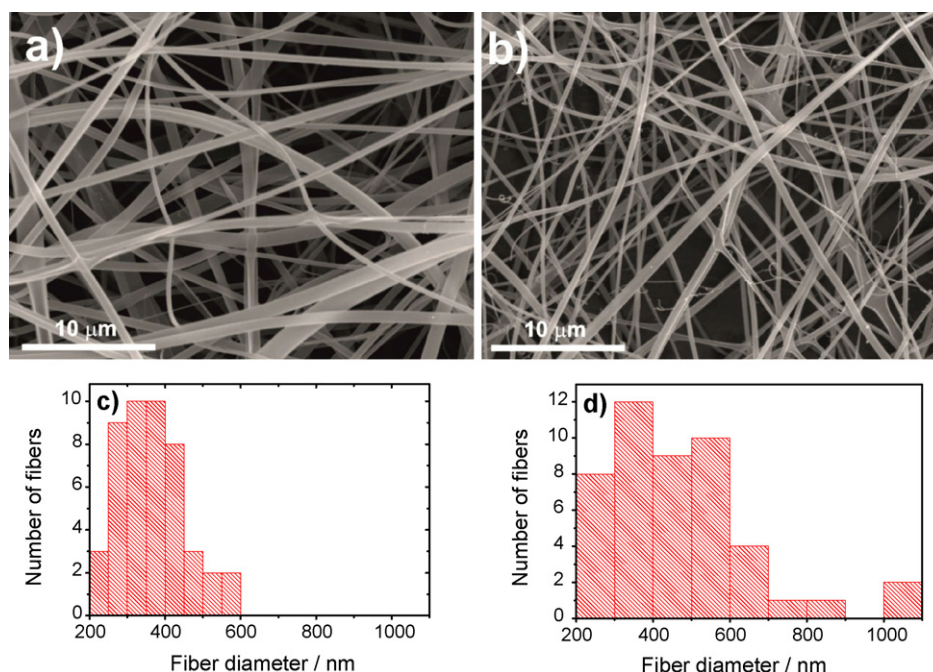


Fig. 2. Morphology of the chitosan mats for the samples obtained with a 7% (w/v) polymer solution at a traveling distance of 150 mm, needle diameter of 0.5 mm, flow rate of 2 ml h⁻¹ and a voltage of 25 kV: (a) 80:20 and (b) 60:40 TFA/DCM (v/v) solution; (c) and (d) represent the fiber diameter histograms of the corresponding figures.

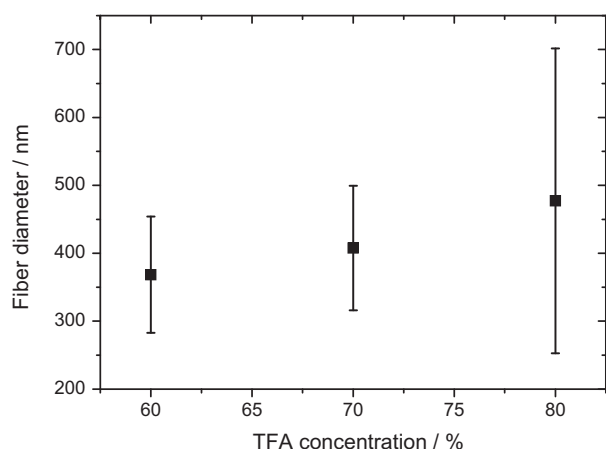


Fig. 3. Influence of the TFA/DCM volume ratio in the distribution of fiber diameters in the electrospun mats obtained for a 7% (w/v) chitosan solution at a fixed traveling distance of 150 mm, needle diameter of 0.5 mm, flow rate of 2 ml h⁻¹ and a voltage of 25 kV.

This fact can be attributed to the lower DCM solvent evaporation temperature (Fig. 4). On the other hand, the samples obtained with a higher needle diameter show a more uniform fiber size distribution. It was also noted that all samples were free of beads, indicating that the tested chitosan electrospinning conditions provide sufficient chain entanglement for fiber formation.

The presence of small particles (Fig. 4b) on the surface of the electrospun fibers has been explained by Zhang et al. as a consequence of the presence of salts (Zhang, Yuan, Wu, Han, & Sheng, 2005) originated by the chitosan dissolution in the TFA acid, as explained above. These salts are commonly observed for higher polymer concentrations and higher TFA content in the chitosan-TFA/DCM solvent solution.

The average size of the fibers for the different needle inner diameters was calculated and the results show a slight increase of the

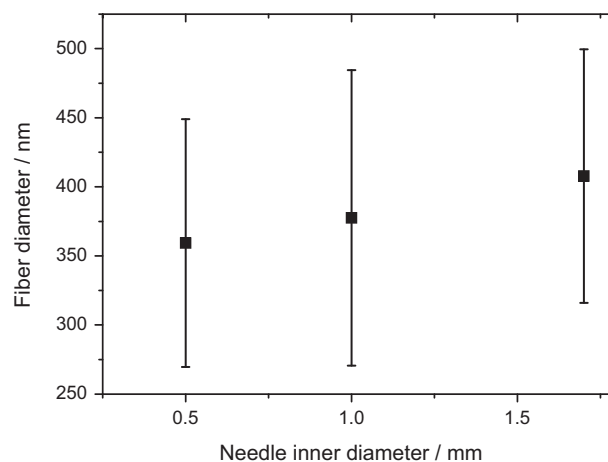


Fig. 5. Influence of the inner diameter of the needle in the average fiber diameter and distribution for the electrospun mats obtained for a 7% (w/v) chitosan solution, a 70/30 TFA/DCM solvent solution, a traveling distance of 150 mm, flow rate of 2 ml h⁻¹ and a voltage of 25 kV.

average fiber diameter from ~360 to 410 nm with increasing inner needle diameter (Fig. 5).

The fiber diameter distribution along the sample is quite similar for all the electrospun samples, being therefore independent of the needle inner diameter. Literature shows contradictory results in this point. Macossay et al. found no influence of the needle diameter on the average fiber diameter of poly(methyl methacrylate) electrospun fibers (Macossay, Marruffo, Rincon, Eubanks, & Kuang, 2007), while Katti et al. and Ribeiro et al. reported that the fiber diameter decreases with decreasing needle inner diameter (Katti, Robinson, Ko, & Laurencin, 2004; Ribeiro, Sencadas, Ribelles, & Lanceros-Méndez, 2010).

A decrease of the inner diameter of the needle causes a reduction of the droplet at the tip and therefore the surface tension of the droplet increases. Then, for a given applied voltage, a larger

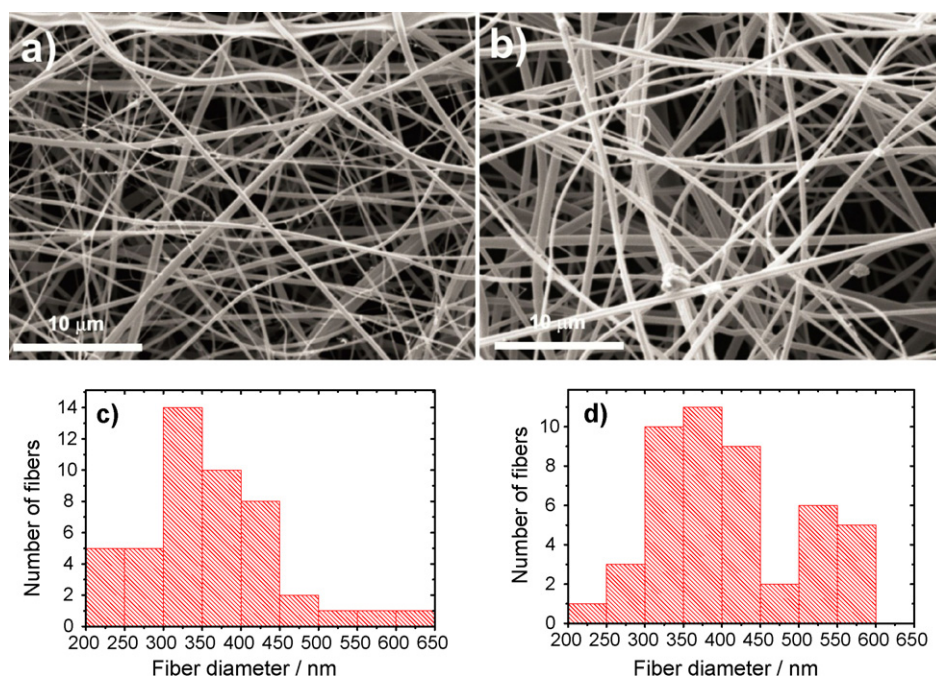


Fig. 4. Morphology of the chitosan mats for the samples obtained for a 7% (w/v) polymer solution, a 70/30 TFA/DCM solvent solution, a traveling distance of 150 mm, flow rate of 2 ml h⁻¹ and a voltage of 25 kV for needle inner diameters of (a) 0.5 mm and (b) 1.7 mm; (c) and (d) represent the fiber diameter histograms of the corresponding figures.

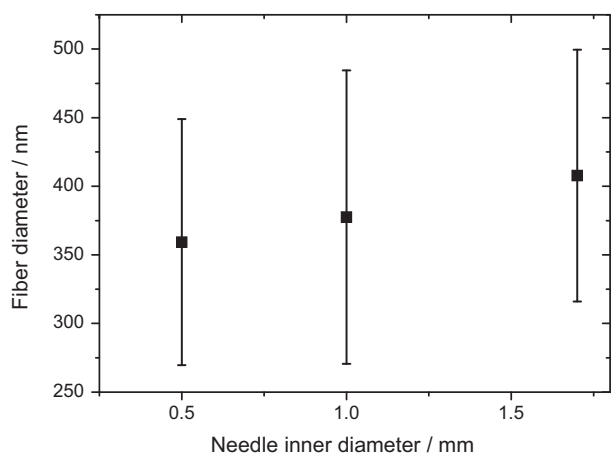


Fig. 6. Influence of the traveling distance on the fiber average diameter and distribution in the electrospun mats obtained for a 7% (w/v) chitosan solution, a 70/30 TFA/DCM solvent solution, a needle inner diameter of 0.5 mm, a flow rate of 2 ml h⁻¹ and a voltage of 25 kV.

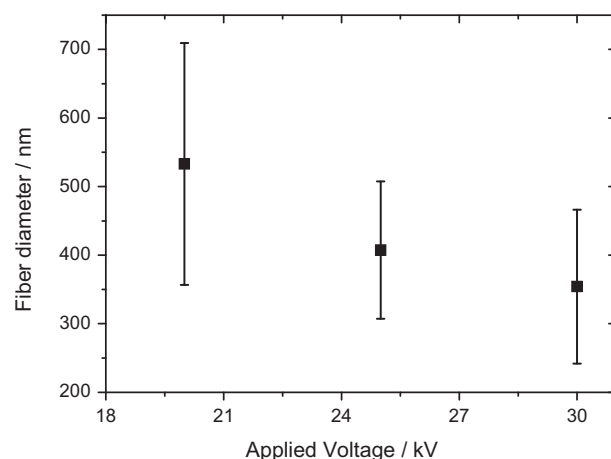


Fig. 8. Influence of the applied voltage on fiber average diameter and distribution in the electrospun mats obtained for a 7% (w/v) chitosan solution, a 70/30 TFA/DCM solvent solution, needle inner diameter of 1.7 mm, flow rate of 2 ml h⁻¹ and a traveling distance of 15 cm.

Coulombic force is required to cause the jet initiation, which results in a decrease of the jet acceleration and, as a consequence, more time is required for the solution to be stretched and elongated before it is collected (Ramakrishna et al., 2005).

The influence of the distance between the needle tip to the grounded collector on the fiber average diameter and distribution was also analyzed. It was observed that the fibers with the smallest average diameter, ~260 nm, were obtained for the samples with a 50 mm distance between the needle tip and the collector and that the mean fiber diameter increases by increasing the distance between the needle tip and the collector. A maximum average fiber diameter of ~500 nm was obtained for a traveling distance of 200 mm (Fig. 6).

It was also observed that the mean diameter fiber distribution increases with increasing the distance between the needle tip and the sample collector. The presence of sub-structures of smaller fibers between the smooth large fibers (Fig. 7) suggests the formation of a secondary jet during the main electrospinning process due to the high solution viscosity (Fig. 1). Ding et al. (2006) pointed out that this fact is related to certain processing conditions such as high voltage, low relative humidity and fast phase separation of polymer and solvent during the flight between the needle and the collector.

Ramakrishna et al. (2005) justified these structures as a consequence of the formations and ejection of smaller jets from the surface of the primary jets, which is comparable to the ejection of

the initial jet from the surface of a charged droplet. It was proposed that the elongation of the jet and evaporation of the solvent modifies the shape and the charge density of the jet during the traveling between the tip and the collector. Thus, the balance between the electrical forces and surface tension can change, giving rise to instabilities in the shape of the jet. Such instabilities can decrease the local charge per unit surface area by ejecting a smaller jet from the surface of the primary jet or by splitting apart into two smaller jets. In this work a blend of two solvents with different boiling points (Table 1) has been used and the observed sub-structures of smaller fibers can be related to the fast evaporation of the DCM solvent from the blend during the traveling from the needle tip to the collector, leaving behind solidified fibers with smaller diameters than the ones that crystallize later when the TFA solvent evaporates. This phenomenon was also observed in Figs. 2 and 3, when the effect of TFA/DCM solvent ratio on fiber diameter and mat morphology was presented.

It is pointed out that an increase of the distance between the tip and the collector often results in a decrease of the fiber diameter (Ramakrishna et al., 2005). However, in the present work it was observed that the diameter of the fibers increases for increasing distance between the needle tip and the grounded collector. This behavior is to be ascribed to the decrease of the electrostatic field strength resulting in a decrease of the electrostatic force and therefore on the stretching of the fibers.

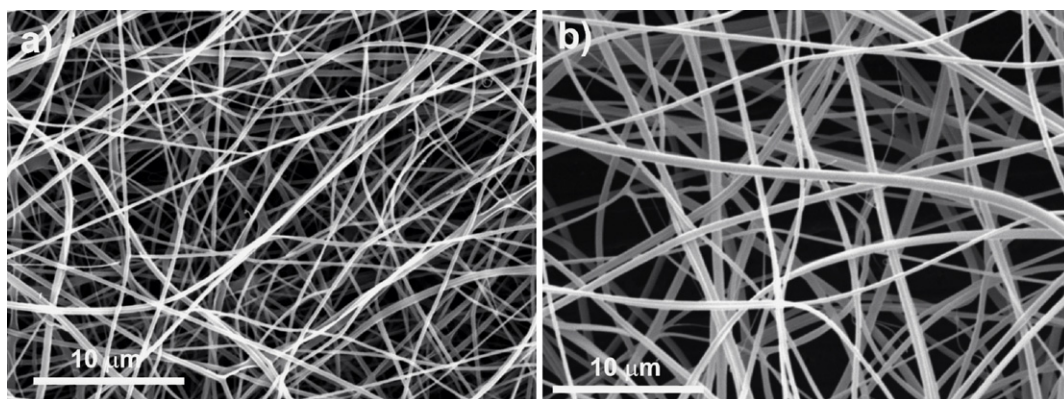


Fig. 7. Morphology of the chitosan mats for the samples obtained for a 7% (w/v) polymer solution, a 70/30 TFA/DCM solvent solution and a needle diameter of 0.5 mm, at a traveling distance of 150 mm, flow rate of 2 ml h⁻¹, a voltage of 25 kV and a distance between the needle tip to the sample collector of (a) 50 mm and (b) 200 mm.

Tip to collector distance has a direct influence on the jet flight time and electric field strength: a decrease of the distance shortens flight and solvent evaporation times and increases the electric field strength. A decrease in the tip to collector distance has a similar effect as increasing the voltage (Fig. 8).

The changes in the applied electric field have strong influence on the shape of the droplet at the needle tip, its surface charge, dripping rate, velocity of the flowing fluid and hence on the fiber structure and morphology. Similarly, the needle tip to collector distance also determines the time available for fiber drying and the space available for fiber splaying and whipping to take place.

The high voltage will induce the necessary charge distribution on the solution and initiate the electrospinning process when the electrostatic force overcomes the surface tension of the solution (Ramakrishna et al., 2005). For higher electric fields, the jet will accelerate and stretch due to the larger Coulombic forces, which results in a reduction of the fiber average diameter and also promotes faster solvent evaporation to yield drier fibers (Ramakrishna et al., 2005).

Finally, the influence of the feed rate on the average fiber distribution was characterized (Fig. 9). A minimum value of solution volume suspended at the end of the needle should be maintained in order to form a stable Taylor cone (Teo & Ramakrishna, 2006). The feed rate determines the amount of solution available for the electrospinning process. Typically, when the feed rate increases, a corresponding increase of the fiber diameter is observed, as observed i.e. for poly(vinylidene fluoride) (Ribeiro, Sencadas, Ribelles, & Lanceros-Méndez, 2010) and for poly(L-lactide acid) (Ribeiro et al., 2011). In chitosan such behavior was not found and the fiber diameter distribution is quite similar for the different feed rates within the range studied in the present work (Fig. 9).

It was expected that increasing feed rate will increase the volume of the solution drawn from the needle tip, and consequently the jet would take a longer time to dry. The lower boiling point of the solvents used in this work (Table 1) allows the fast

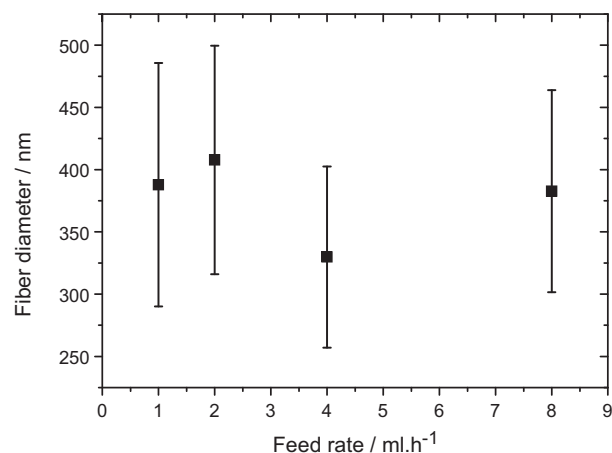


Fig. 9. Influence of the feed rate on the average fiber diameter and distribution of the electrospun mats obtained for a 7% (w/v) chitosan solution, a 70/30 TFA/DCM solvent solution, needle inner diameter of 0.5 mm, flow rate of 2 ml h⁻¹, a traveling distance of 15 cm and a 25 kV applied voltage.

evaporation during the flight time. In this situation, full solvent evaporation has already occurred when the fiber reaches the grounded collector and therefore the feed rate does not have influence on the fiber diameter.

Most of the physical and chemical properties of this biopolymer strongly depend on the degree of deacetylation (DD) (Lavertu et al., 2003). The DD can be calculated from the ¹H NMR spectra (Fig. 10) through:

$$DD(\%) = \frac{H_1 D}{H_1 D + (H_{ac}/3)} \times 100$$

where H₁D is the peak corresponding to the H₁ proton of the deacetylated monomer (duplet at δ = 4.858 ppm) and H_{ac} is the peak of the three protons of the acetyl group (singlet at δ = 1.988 ppm)

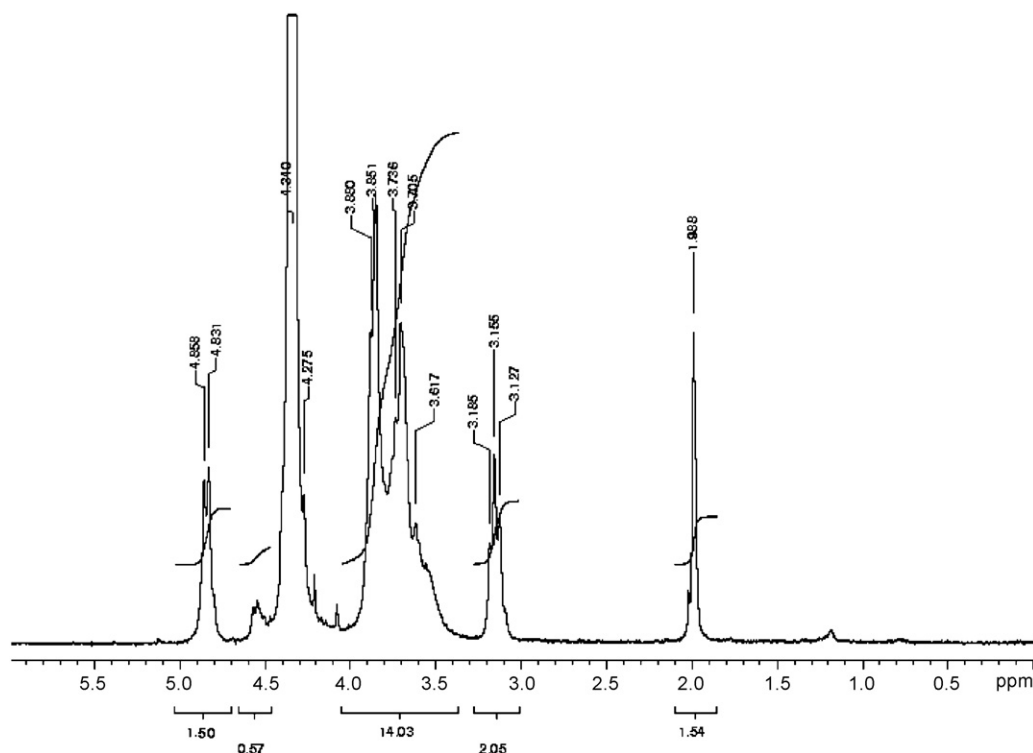


Fig. 10. ¹H NMR spectra of electrospun chitosan nanofibers at 70 °C.

(Lavertu et al., 2003). The obtained results show that the commercial chitosan has a DD of 78%, which is similar to the value given by the producer and also similar to the values obtained for the electrospun fibers. It is therefore concluded that the electrospinning process does not affect the degree of deacetylation of the polymer.

4. Conclusions

Large chitosan mats with uniform fibers of submicron diameters without beads have been prepared from trifluoroacetic acid/dichloromethane mixture solutions by a stable electrospinning process. It was observed that an increase of the DCM present in the solvent blend solution produces nanofibers with smaller diameters and narrower diameter distribution. Inclusion of DCM within the TFA solutions modifies solution viscosity and electrical characteristics, leading to a stable flow rate and avoiding spark formation. The inner diameter of the needle and the feed rate does not have influence in the chitosan electrospun fiber diameter. On the other hand, it was observed that a decrease of the distance from the needle tip to the grounded collector gives origin to nanofibers with smaller diameters. Finally, an increase of the applied voltage also decreases the nanofibers diameter. The degree of deacetylation of the polymer is not affected by the electrospinning process.

Acknowledgements

This work is funded by FEDER funds through the “Programa Operacional Factores de Competitividade – COMPETE” and by national funds by FCT – Fundação para a Ciência e a Tecnologia, project references NANO/NMed-SD/0156/2007. VS thanks the FCT for the SFRH/BPD/63148/2009 grants. JLGR acknowledge the support of the Spanish Ministry of Science and Innovation through project No. MAT2010-21611-C03-01 (including the FEDER financial support) and Programa Nacional de Internacionalización de la I+D project EUI2008-00126. Funding for research in the field of Regenerative Medicine through the collaboration agreement from the Conselleria de Sanidad (Generalitat Valenciana), and the Instituto de Salud Carlos III (Ministry of Science and Innovation) is also acknowledged.

Thanks are due to the National NMR Network that was purchased within the framework of the National Program for Scientific Re-equipment, contract REDE/1517/RMN/2005 with funds from POCI 2010 (FEDER) and FCT. Also thank to the UPV Microscopy Service for the use of their lab.

References

- Baldrick, P. (2010). The safety of chitosan as a pharmaceutical excipient. *Regulatory Toxicology and Pharmacology*, 56(3), 290–299.
- Beachley, V. & Wen, X. (2010). Polymer nanofibrous structures: Fabrication, biofunctionalization, and cell interactions. *Progress in Polymer Science*, 35(7), 868–892.
- Bhardwaj, N. & Kundu, S. C. (2010). Electrospinning: A fascinating fiber fabrication 354 technique. *Biotechnology Advances*, 28(3), 325–347.

- Budavari, S. (1996). *An encyclopedia of chemicals, drugs and biologicals*. New Jersey: Merck & Co.
- Ribeiro, C., et al. (2011). Tailoring the morphology and crystallinity of poly(L-lactide acid) electrospun membranes. *Science and Technology of Advanced Materials*, 12(1), 015001.
- Dannhauser, W. & Cole, R. H. (1952). On the dielectric constant of trifluoroacetic acid. *Journal of the American Chemical Society*, 74(23), 6105.
- Ding, B., et al. (2006). Formation of novel 2D polymer nanowebs via electrospinning. *Nanotechnology*, 17(15), 3685.
- Fernandez-Megia, E., Novoa-Carballal, R., Quiñoá, E. & Riguera, R. (2005). Optimal routine conditions for the determination of the degree of acetylation of chitosan by ¹H NMR. *Carbohydrate Polymers*, 61(2), 155–161.
- Honarkar, H. & Barikani, M. (2009). Applications of biopolymers I: Chitosan. *Monatshefte Fur Chemie*, 140(12), 1403–1420.
- Image J. (2011). *Image processing and analysis in Java*. Available from: <http://rsbweb.nih.gov/ij/index.html>.
- Jayakumar, R., Menon, D., Manzoor, K., Nair, S. V. & Tamura, H. (2010). Biomedical applications of chitin and chitosan based nanomaterials – A short review. *Carbohydrate Polymers*, 82(2), 227–232.
- Jayakumar, R., Prabakaran, M., Nair, S. V. & Tamura, H. (2010). Novel chitin and chitosan nanofibers in biomedical applications. *Biotechnology Advances*, 28(1), 142–150.
- Jayakumar, R., Prabakaran, M., Nair, S. V., Tokura, S., Tamura, H. & Selvamurugan, N. (2010). Novel carboxymethyl derivatives of chitin and chitosan materials and their biomedical applications. *Progress in Materials Science*, 55(7), 675–709.
- Jayakumar, R., Prabakaran, M., Sudheesh Kumar, P. T., Nair, S. V. & Tamura, H. (2011). Biomaterials based on chitin and chitosan in wound dressing applications. *Biotechnology Advances*, 29(3), 322–337.
- Katti, D. S., Robinson, K. W., Ko, F. K. & Laurencin, C. T. (2004). Bioresorbable nanofiber-based systems for wound healing and drug delivery: Optimization of fabrication parameters. *Journal of Biomedical Materials Research. Part B: Applied Biomaterials*, 70B(2), 286–296.
- Krajewska, B. (2005). Membrane-based processes performed with use of chitin/chitosan materials. *Separation and Purification Technology*, 41(3), 305–312.
- Lavertu, M., Xia, Z., Serreqi, A. N., Berrada, M., Rodrigues, A., Wang, D., et al. (2003). A validated ¹H NMR method for the determination of the degree of deacetylation of chitosan. *Journal of Pharmaceutical and Biomedical Analysis*, 32(6), 1149–1158.
- Macossay, J., Marruffo, A., Rincon, R., Eubanks, T. & Kuang, A. (2007). Effect of needle diameter on nanofiber diameter and thermal properties of electrospun poly(methyl methacrylate). *Polymers for Advanced Technologies*, 18(3), 180–183.
- Malafaya, P. B., Silva, G. A. & Reis, R. L. (2007). Natural-origin polymers as carriers and scaffolds for biomolecules and cell delivery in tissue engineering applications. *Advanced Drug Delivery Reviews*, 59(4–5), 207–233.
- Ohkawa, K., Cha, D., Kim, H., Nishida, A. & Yamamoto, H. (2004). Electrospinning of chitosan. *Macromolecular Rapid Communications*, 25(18), 1600–1605.
- Pillai, C. K. S., Paul, W. & Sharma, C. P. (2009). Chitin and chitosan polymers: Chemistry, solubility and fiber formation. *Progress in Polymer Science*, 34(7), 641–678.
- Ravi Kumar, M. N. V. (2000). A review of chitin and chitosan applications. *Reactive and Functional Polymers*, 46(1), 1–27.
- Ribeiro, C., Sencadas, V., Ribelles, J. L. G. & Lanceros-Méndez, S. (2010). Influence of processing conditions on polymorphism and nanofiber morphology of electroactive poly(vinylidene fluoride) electrospun membranes. *Soft Materials*, 8(3), 274–287.
- Ramakrishna, S., Fujihara, K., Teo, W. E., Lim, T. C. & Ma, Z. (2005). *Introduction to electrospinning and nanofibers*. Singapore: World Scientific.
- Schiffman, J. D. & Schauer, C. L. (2006). Cross-linking chitosan nanofibers. *Biomacromolecules*, 8(2), 594–601.
- Schiffman, J. D. & Schauer, C. L. (2007). One-step electrospinning of cross-linked chitosan fibers. *Biomacromolecules*, 8(9), 2665–2667.
- Sill, T. J. & von Recum, H. A. (2008). Electrospinning: Applications in drug delivery and tissue engineering. *Biomaterials*, 29(13), 1989–2006.
- Teo, W. E. & Ramakrishna, S. (2006). A review on electrospinning design and nanofiber assemblies. *Nanotechnology*, 17(14), R89.
- Yaghobi, N. & Hormozi, F. (2010). Multistage deacetylation of chitin: Kinetics study. *Carbohydrate Polymers*, 81(4), 892–896.
- Zhang, C., Yuan, X., Wu, L., Han, Y. & Sheng, J. (2005). Study on morphology of electrospun poly(vinyl alcohol) mats. *European Polymer Journal*, 41(3), 423–432.